

Population pharmacokinetic-pharmacodynamic model of  
oxfendazole in healthy adults in a multiple ascending dose  
and food effect study and target attainment analysis

Thanh Bach<sup>a</sup>, Gregory A. Deye<sup>b</sup>, Ellen E. Codd<sup>c,d</sup>, John Horton<sup>d,e</sup>, Patricia Winokur<sup>f</sup>, Guohua  
An<sup>a,#</sup>

<sup>a</sup>Division of Pharmaceutics and Translational Therapeutics, College of Pharmacy, University of  
Iowa, Iowa City, Iowa, USA

<sup>b</sup> Division of Microbiology and Infectious Diseases, National Institute of Allergy and Infectious  
Diseases, Bethesda, Maryland, USA

<sup>c</sup>Codd Consulting, LLC, Blue Bell, Pennsylvania, USA

<sup>d</sup>Oxfendazole Development Group, Blue Bell, Pennsylvania, USA

<sup>e</sup>Tropical Projects, Hitchin, UK

<sup>f</sup> Division of Infectious Diseases, Carver College of Medicine, University of Iowa, Iowa City,  
Iowa, USA

<sup>#</sup>Corresponding author:

Guohua An, MD, PhD

Division of Pharmaceutics and Translational Therapeutics

University of Iowa, College of Pharmacy

115 S Grand Ave, Iowa City, IA, 52242, USA

Tel: (319) 467-4600; E-mail: [guohua-an@uiowa.edu](mailto:guohua-an@uiowa.edu)

**Running title:** Oxfendazole popPKPD model and target attainment analysis

28 **ABSTRACT**

29 Oxfendazole is a potent veterinary antiparasitic drug undergoing development for human use to  
30 treat multiple parasitic infections. Results from two recently completed Phase I clinical trials  
31 conducted in healthy adults showed that the pharmacokinetics of oxfendazole is nonlinear,  
32 affected by food, and, after the administration of repeated doses, appeared to mildly affect  
33 hemoglobin concentrations. To facilitate oxfendazole dose optimization for its use in patient  
34 populations, the relationship among oxfendazole dose, pharmacokinetics and hemoglobin  
35 concentration was quantitatively characterized using population pharmacokinetic-  
36 pharmacodynamic modeling. In fasting subjects, oxfendazole pharmacokinetics was well  
37 described by a one-compartment model with first-order absorption and elimination. The change  
38 in oxfendazole pharmacokinetics when administered following a fatty meal was captured by an  
39 absorption model with one transit compartment and increased bioavailability. The effect of  
40 oxfendazole exposure on hemoglobin concentration in healthy adults was characterized by a  
41 lifespan indirect response model in which oxfendazole has positive but minor inhibitory effect on  
42 red blood cell synthesis. Further simulation indicated that oxfendazole has a low risk of posing a  
43 safety concern regarding hemoglobin concentration, even at a high oxfendazole dose of 60  
44 mg/kg once daily. The final model was further used to perform comprehensive target attainment  
45 simulations for whipworm infection and filariasis at various dose regimens and target attainment  
46 criteria. The results of our modeling work, when adopted appropriately, have the potential to  
47 greatly facilitate oxfendazole dose regimen optimization in patient populations with different  
48 types of parasitic infections.

## 1 INTRODUCTION

Neglected tropical diseases are a diverse set of infections caused by bacteria, viruses, protozoa, and metazoan that affect more than 1.5 billion people worldwide(1). Even though some neglected tropical diseases have been effectively controlled and almost eradicated, there remain multiple difficult-to-treat infections, which include neurocysticercosis, trichuriasis, echinococcosis, fascioliasis, and filariasis. Although these diseases are currently treated by the benzimidazole anthelmintic drugs albendazole, mebendazole, or triclabendazole, these treatments are not optimal due to their low efficacy(2-5), drug resistance(6), and/or unfavorable pharmacokinetics (e.g. short and greatly variable half-life)(7-9).

Oxfendazole is a potent benzimidazole anthelmintic marketed to treat lungworm and enteric helminths in animals(10). A single oral low dose of oxfendazole effectively reduced worm burden in *Trichuris suis* infected pigs(11, 12), a surrogate model of human whipworm infection. In filaria infected mice, orally or subcutaneously administered oxfendazole demonstrated up to 100% macrofilaricidal efficacy at a dosing regimen of 25 mg/kg daily for 5 days(13). The preclinical efficacy of oxfendazole in the treatment of neurocysticercosis, echinococcosis, and fascioliasis were presented in detail in a recent review(14). These results suggest that oxfendazole is a potential candidate for the treatment of multiple parasitic infections in humans. This is further supported by the favorable safety(10, 15) and pharmacokinetic profiles of oxfendazole in preclinical species. Oxfendazole exposure and half-life were greater than or comparable to those of albendazole and mebendazole in dogs(16), sheep(17), pigs(18, 19), and rats(15, 20).

Previously, the safety, tolerability, and pharmacokinetics of oxfendazole and its metabolites in healthy adults were evaluated following oral administration of single ascending oxfendazole

72 doses between 0.5 and 60 mg/kg(21). In that study, oxfendazole was the major moiety detected  
73 in plasma, followed by oxfendazole sulfone and fenbendazole(21). The same relative systemic  
74 exposure to parent drug and metabolites was observed in pigs(22), supporting their use as an  
75 appropriate preclinical model for oxfendazole toxicity and efficacy. In a disposition study of  
76 oxfendazole in *T. suis* infected pigs, the oxfendazole concentration in whipworm tissue was  
77 highly correlated to the drug's concentration in pig plasma(22), suggesting that plasma is a  
78 significant route for oxfendazole access to whipworm. Further, in humans, the dose-normalized  
79 exposure of oxfendazole was 27 times higher than that of albendazole and 538 times higher than  
80 that of mebendazole(23-25). Taken together, these data suggest that oxfendazole has an  
81 advantageous pharmacokinetic profile compared to those of albendazole and mebendazole for  
82 the treatment of whipworm infection in humans.

83 Given the encouraging results from the single ascending dose oxfendazole clinical trial, we  
84 recently completed and published the results of the second clinical trial assessing oxfendazole  
85 safety, tolerability, and pharmacokinetics in healthy adults following the administration of  
86 multiple ascending doses from 3 to 15 mg/kg (ClinicalTrials.gov ID: NCT03035760)(23). In  
87 healthy adults, oxfendazole absorption was rapid with a time to maximum concentration ( $T_{max}$ )  
88 of ~2 h. Oxfendazole elimination half-life (9.21 – 11.8 h) was consistent across dose groups and,  
89 following the administration of multiple doses at 24 h intervals, oxfendazole plasma levels  
90 reached steady state on Day 3 with little accumulation (accumulation ratio: 0.970 – 1.27).  
91 Oxfendazole exhibited substantial nonlinear pharmacokinetics with a less than dose-proportional  
92 increase in plasma exposure with escalating doses, most likely due to oxfendazole's low  
93 solubility, which caused a decrease a bioavailability with increasing doses. When oxfendazole  
94 was administered following a high-fat breakfast, oxfendazole's peak concentration ( $C_{max}$ )

95 increased 1.49 times and the  $T_{\max}$  increased by 6.88 h compared to those in the fasted state. A  
96 mild decrease in hemoglobin concentration with increasing oxfendazole dose was observed,  
97 although hemoglobin concentrations remained within the normal range for most subjects.

98 Because oxfendazole concentration in plasma is related to both efficacy and potential  
99 hematologic effects, an insight into the correlation between oxfendazole dose and exposure is  
100 important for dose optimization. However, oxfendazole nonlinear pharmacokinetics makes  
101 correlation of oxfendazole dose to exposure difficult. Therefore, in this study, we performed a  
102 secondary analysis of oxfendazole pharmacokinetics and its effect on hemoglobin concentration  
103 using the population pharmacokinetic-pharmacodynamic (popPK/PD) modeling approach.

104 Because a popPK/PD model describes the underlying system, once developed, the model can be  
105 used to predict oxfendazole PK/PD with new dosing regimens that have not been evaluated in  
106 humans, as well as applied to other efficacy endpoints. Thus, we have applied the developed  
107 popPK/PD model of oxfendazole to predict 1) the change in hemoglobin concentration following  
108 multiple ascending doses from 3 to 60 mg/kg, and 2) the probability of target attainment of  
109 oxfendazole in treating whipworm infection and filariasis in humans.

## 110 2 RESULTS

### 111 2.1 Population pharmacokinetic-pharmacodynamic model

#### 112 2.1.1 Structural model

##### 113 *Pharmacokinetic model*

114 Structural pharmacokinetic models for oxfendazole in the fasted state and fed state are presented  
115 in **Figure 1A** and **Figure 1B**, respectively. The prolonged absorption of oxfendazole in the fed  
116 state was best captured by an absorption model with 1 transit compartment.

##### 117 *Pharmacodynamic model*

118 Two models were examined to characterize the decrease in hemoglobin concentration with  
119 multiple ascending oxfendazole doses: 1) the basic indirect response model with inhibition of  
120 hemoglobin synthesis and 2) the lifespan indirect response model with inhibition of red blood  
121 cell synthesis. The two models performed similarly well based on Akaike Information Criterion  
122 (AIC), parameter feasibility and precision, and goodness-of-fit plots. The more mechanistic  
123 lifespan model (**Figure 1A**) was chosen as the final structural pharmacodynamic model because  
124 it is known that red blood cells are cleared after an average of 120 days in adults (i.e., they have  
125 relatively consistent lifespan). In this model, oxfendazole's inhibitory effect on hemoglobin  
126 synthesis was linearly correlated to oxfendazole concentration in plasma.

#### 127 2.1.2 Stochastic model

128 Inter-individual and inter-occasion variability of all pharmacokinetic parameters were  
129 investigated. Inter-individual variability in transit rate constant ( $k_{TR}$ ), absorption rate constant  
130 ( $k_a$ ), oxfendazole apparent volume of distribution ( $V_{OXF}$ ), oxfendazole apparent clearance

131 ( $CL_{OXF}$ ), and hemoglobin synthesis rate constant ( $k_{in}$ ), and inter-occasion variability in  $V_{OXF}$  and  
132  $CL_{OXF}$  were significant.

### 133 2.1.3 Covariate model

134 None of the evaluated covariates had significant impact on oxfendazole pharmacokinetics. Sex  
135 significantly affected  $k_{in}$ , with  $k_{in}$  in females being 91.3% (95% confidence interval: 90.8 –  
136 91.8%) of that in males (**Table 1**).

### 137 2.1.4 Model evaluation

138 Model evaluation based on goodness-of-fit plots indicated no systemic bias in terms of  
139 oxfendazole plasma concentration (**Supplementary Figure S1**) or hemoglobin concentration  
140 (**Supplementary Figure S2**). **Figure 2** presents the time course of population predicted  
141 oxfendazole concentrations versus the mean observed oxfendazole concentrations following the  
142 administration of multiple ascending doses (upper panel) or a single dose in fasted and fed states  
143 (lower panel). The change in population predicted hemoglobin concentration versus change in  
144 observed hemoglobin concentration after the administration of multiple oxfendazole doses is  
145 presented in **Figure 3**. Overall, there was good agreement between model predicted and  
146 observed data under all dosing regimens and conditions, indicating that the model was sufficient  
147 at capturing oxfendazole PK/PD.

148 Final estimates of model parameters are summarized in **Table 1**. Relative standard error (%RSE)  
149 was <30% for all PK/PD parameters, suggesting that all PK/PD parameters were estimated with  
150 good precision. The estimated variance of inter-individual variability in  $k_a$ ,  $k_{TR}$ , and  $V_{OXF}$  had  
151 %RSE of more than 50%. However, removal of these inter-individual variability terms  
152 negatively impacted model performance. Condition numbers (ratio of the highest to the lowest  
153 eigenvalue) were 269.3 for the final pharmacokinetic model and 1.6 for the final

154 pharmacodynamic model. Condition numbers being less than 1000 indicate that the model is not  
155 ill-conditioned or over-parameterized.

156 Model predictive performance was evaluated using prediction-corrected visual predictive check  
157 as presented in **Figure 4** for all dose groups and in **Supplemental Figure S4** and **S5** for each  
158 dose group. Based on these figures, the observed 5<sup>th</sup>, 50<sup>th</sup> and 95<sup>th</sup> percentiles were within 95%  
159 confidence interval of the respective simulated percentiles, suggesting that the final popPK/PD  
160 model for oxfendazole and its effect on hemoglobin concentrations had good predictive  
161 performance.

## 162 2.2 Simulation

### 163 2.2.1 Simulation of exposure-response on safety

164 To investigate the maximal decrease in hemoglobin concentrations following the administration  
165 of multiple ascending oxfendazole doses, hemoglobin concentrations in healthy subjects were  
166 simulated following the administration of multiple ascending oxfendazole doses at 3, 7.5, 15, 30,  
167 and 60 mg/kg once daily for 5 days and compared to the normal range and toxicity grade 1 – 3  
168 ranges of hemoglobin in adults. Among the simulated doses, 3 – 15 mg/kg were evaluated in  
169 oxfendazole multiple ascending dose trial, and 30 – 60 mg/kg doses were evaluated in the single  
170 ascending dose trial. The simulation did not include doses higher than 60 mg/kg because  
171 oxfendazole exposure is saturated due to dose-limited bioavailability(21).

172 Simulated hemoglobin concentrations following the administration of multiple ascending doses  
173 of oxfendazole to males and females are presented in **Figure 5**. According to the lifespan model,  
174 baseline hemoglobin concentration is a product of  $T_R$  and  $k_{in}$ . Because inter-individual variability  
175 in  $T_R$  was fixed to 0, the variability in simulated hemoglobin concentration at baseline was due to  
176 inter-individual variability of  $k_{in}$  (**Table 1**). Although the magnitude of the decrease in



177 hemoglobin concentration increased with ascending oxfendazole doses (**Figure 5**), the median  
178 hemoglobin concentration remained in the normal range at all dose levels.

## 179 **2.2.2 Simulation of exposure-response on efficacy**

### 180 Target attainment analysis for whipworm infection – approach #1

181 In the first approach to target attainment analysis for whipworm infection, an  $IC_{50} = 480$  ng/mL  
182 was estimated as the concentration of oxfendazole in plasma that resulted in 50% inhibition of  
183 tubulin assembly in whipworm. (Detailed derivation of this concentration is described in the  
184 [Methods](#) section.)

185 If 100% of adult whipworms are eliminated from the body when peak concentration at steady  
186 state ( $C_{max,ss}$ ) is equal to  $IC_{50}$ , 100% of the patients would be cured even at the lowest simulated  
187 dose of 0.5 mg/kg (**Figure 6**). If targeted  $C_{max,ss} = 5*IC_{50}$ , 90% target attainment was achieved at  
188 doses  $\geq 7.5$  mg/kg. At targeted  $C_{max,ss} = 10*IC_{50}$ , 90% target attainment was achieved at doses  
189  $\geq 50$  mg/kg. At targeted  $C_{max,ss} \geq 15*IC_{50}$ , probability of target attainment dropped below 70% at  
190 all doses 0.5 – 60 mg/kg.

191 Because whipworm elimination might depend on how long the worm is exposed to oxfendazole,  
192 target attainment analysis was additionally performed based on  $T_{>IC_{50}}$  (i.e., the percent time of a  
193 dosing interval (24 h) at steady state during which oxfendazole concentration is above  $IC_{50}$ ), and  
194 the results are summarized in **Table 2**. According to **Table 2**, if maintenance of oxfendazole  
195 concentration above  $IC_{50}$  ( $T_{>IC_{50}} = 100\%$ ) is required for complete whipworm elimination, 90%  
196 of the patients would be completely cured at oxfendazole doses of 30 – 60 mg/kg. If  $T_{>IC_{50}} \geq$   
197 80% is taken as the criteria for complete deworming, 90% target attainment is reached at doses

198 above 5 mg/kg. At  $T_{>IC_{50}} \geq 60\%$ , 90% target attainment is achievable at doses above 4 mg/kg. At  
199  $T_{>IC_{50}} \geq 40\%$ , 90% target attainment is possible at doses as low as 1 mg/kg.

200 Target attainment analysis for whipworm infection – approach #2

201 In the second approach to target attainment analysis for whipworm infection,  $IC_{50} = 5290$  ng/mL  
202 was estimated as the concentration of oxfendazole in plasma at which 50% of adult whipworms  
203 are killed. (Rationales for the proposed  $IC_{50}$  is discussed in the [Methods](#) section.)

204 Assuming that whipworm elimination depends on oxfendazole  $C_{max,ss}$ , to achieve 100% cure rate,  
205  $C_{max,ss}$  must be higher than  $IC_{50}$  of 5290 ng/mL. According to **Figure 7**, the probability of target  
206 attainment was less than 90% for all doses other than the 60 mg/kg dose. **Table 3** presents the  
207 probability of target attainment based on  $T_{>IC_{50}}$ . For  $T_{>IC_{50}} \geq 40\%$ , probability of target  
208 attainment is less than 50% at all doses (0.5 – 60 mg/kg).

209 Target attainment analysis for filariasis

210 Based on a mouse model of filariasis, the macrofilaricidal effect (i.e., killing of adult worms) of  
211 oxfendazole is driven by the maintenance of the minimal efficacious concentration (MEC) of  
212 100 ng/mL in plasma. To account for uncertainty extrapolating exposure-response data from  
213 mouse to human, target attainment analysis was performed at different MEC values ranging from  
214 100 to 4000 ng/mL. The mean simulated concentration-time profile of oxfendazole in human  
215 plasma following multiple ascending doses (0.5 – 60 mg/kg once daily for 5 days) compared to  
216 different MEC levels are presented in **Figure 8A**, and the probability of target attainment at  
217 different MEC values and dosing regimens are presented in **Figure 8B**. According to **Figure 8A**,  
218 the mean concentrations of oxfendazole at all doses are above MEC throughout the dosing  
219 interval given MEC = 100 and 200 ng/mL. Correspondingly, **Figure 8B** demonstrates that the

220 probability of target attainment at MEC = 100 ng/mL is in the range of 90 – 100% under all  
221 dosing regimens. At MEC = 200 ng/mL, probability of target attainment is  $\geq 90\%$  at doses of at  
222 least 3 mg/kg. At MEC = 500 ng/mL, 90% target attainment is achieved only at doses of 30  
223 mg/kg and above. At MEC = 1000 ng/mL and 1500 ng/mL, even the highest doses (50 and 60  
224 mg/kg) can reach only ~75% and 50% target attainment, respectively. At MEC  $\geq 2000$  ng/mL,  
225 none of the simulated dose can pass 50% target attainment.

226

227 **3 DISCUSSION**

228 We have successfully developed a popPK/PD model characterizing oxfendazole  
229 pharmacokinetics and its effect on hemoglobin concentrations in healthy adults in a multiple  
230 ascending dose and food effect evaluation study. Oxfendazole nonlinear pharmacokinetics,  
231 attributed to oxfendazole's low solubility, was modeled with dose-dependent bioavailability. The  
232 delay in oxfendazole absorption, as well as the increase in oxfendazole exposure in the fed  
233 compared to the fasted state were sufficiently captured by the addition of one transit  
234 compartment and increase in bioavailability, respectively. According to the model estimated  
235 parameters (**Table 1**), oxfendazole bioavailability reduced significantly (22 times) as the dose  
236 increased from 0.5 mg/kg to 60 mg/kg. Based on the model developed, oxfendazole's apparent  
237 volume of distribution and apparent clearance at the lowest dose were estimated to be 34.5 L and  
238 2.57 L/h (**Table 1**), respectively, indicating that oxfendazole distribution is moderate and  
239 oxfendazole hepatic extraction is low. A previous non-compartmental analysis showed that in  
240 subjects who have consumed a fatty meal, oxfendazole AUC increased 1.86 times and its  $T_{\max}$   
241 was delayed by 6.88 h(23) compared to those parameters measured in fasting subjects. In  
242 agreement with the published non-compartmental analysis results(23) our present model  
243 estimated a 2.08-fold (**Table 1**) increase in oxfendazole bioavailability in the fed state compared  
244 to the fasted state. In addition, in the fed state, oxfendazole absorption included one transit  
245 compartment with the transit rate constant ( $0.412 \text{ h}^{-1}$ ) being much lower than the absorption rate  
246 constant of oxfendazole in the fasted state ( $1.2 \text{ h}^{-1}$ ) (**Table 1**).

247 The effect of oxfendazole pharmacokinetics on hemoglobin concentration following multiple  
248 doses was sufficiently characterized by a red blood cell lifespan model with  $k_{\text{in}}$  inhibition.  
249 Oxfendazole inhibitory effect on  $k_{\text{in}}$  followed a linear function with linear coefficient of

0.000458 (95% confidence interval: 0.000377 – 0.000539) (**Table 1**). At baseline, hemoglobin  $k_{in}$  in males was estimated to be 0.00509 g/dL/h (equivalent to 0.122 g/dL/day). Hemoglobin  $k_{in}$  in females was 91.3% of that in males (**Table 1**), a result expected considering the lower normal range of hemoglobin concentration observed in females than in males (**Figure 5**). Inter-individual variability in oxfendazole pharmacokinetics and pharmacodynamics were low to moderate, ranging from 6% ( $k_{in}$  inter-individual variability) to 47% ( $k_{TR}$  inter-individual variability) (**Table 1**), which was expected of healthy adult subjects. A limitation of the current pharmacodynamic model is its lack of inclusion of a feedback regulation parameter, thus preventing its use to extrapolate to predict hemoglobin concentration after Day 5.

The developed model was used for exposure-response simulations on safety and efficacy. Regarding oxfendazole safety, simulation of hemoglobin concentration following administration of multiple ascending doses of oxfendazole (3 – 60 mg/kg once daily for 5 days) demonstrated a decrease in hemoglobin concentration with increasing oxfendazole dose (**Figure 5**). However, the median hemoglobin concentrations remained in normal range, with the simulated 5<sup>th</sup> percentile reading into the Grade 1 or Grade 2 toxicity levels. Note the predicted value of the 5<sup>th</sup> percentile is below the normal range prior to the administration of oxfendazole.

In terms of oxfendazole efficacy in the treatment of whipworm infection, four scenarios were explored:  $C_{max,ss} \geq IC_{50} = 480$  ng/mL,  $T_{>IC_{50}} (IC_{50} = 480$  ng/mL),  $C_{max,ss} \geq IC_{50} = 5290$  ng/mL, and  $T_{>IC_{50}} (IC_{50} = 5290$  ng/mL). The two different  $IC_{50}$  values were estimated based on different *in vitro* models with different sets of assumptions as described in the [Methods](#) section.  $C_{max,ss} \geq IC_{50} = 480$  ng/mL was the easiest to achieve target with 100% of the population predicted to meet this requirement even at 0.5 mg/kg dose, and 90% of the population predicted to have oxfendazole concentrations in plasma above 480 ng/mL throughout the dosing interval (i.e.,

273  $T_{>IC_{50}} = 100\%$ ) with 30 – 60 mg/kg dose. In contrast, with  $IC_{50} = 5290$  ng/mL, 90% of the  
274 population is predicted to have  $C_{max,ss} \geq IC_{50} = 5290$  ng/mL only at the highest dose of 60 mg/kg,  
275 and less than 5% of the population maintains an oxfendazole concentration in plasma above  $IC_{50}$   
276  $= 5290$  ng/mL throughout the dosing interval. Increasing the dose over 60 mg/kg would not  
277 improve the probability of target attainment as oxfendazole exposure increased less than dose  
278 proportionally with increasing dose. Due to the lack of exposure-response analysis on  
279 oxfendazole efficacy in treating whipworm infection, target attainment analysis was performed  
280 using two approaches with different sets of assumptions. The two approaches estimated two  $IC_{50}$   
281 values which differed by 11 folds and resulted in dramatically differing probabilities of target  
282 attainment at clinically relevant doses. In addition, with the increase in dose, the change in  
283 efficacy can be very different between  $IC_{50} = 480$  ng/mL and  $IC_{50} = 5290$  ng/mL. At the lower  
284  $IC_{50}$ , increasing dose from 15 to 60 mg/kg was predicted to result in only 10% increase in  
285 probability of target attainment with the target being  $T_{>IC_{50}} = 100\%$ . Meanwhile, at the higher  
286  $IC_{50}$ , increase in dose from 15 to 60 mg/kg was predicted to increase the probability of target  
287 attainment by nearly 30% with the target being  $T_{>IC_{50}} \geq 40\%$ . Thus, results of target attainment  
288 analysis should be considered with caution.

289 For filariasis treatment, assuming that the minimal efficacious concentration of oxfendazole in  
290 mouse (100 ng/mL)(26) and human is the same, 90% target attainment is feasible even at low  
291 dose (0.5 mg/kg).

292 The *in vitro* study monitoring adult *T. muris* motility in culture as an indication of live worms  
293 reported  $IC_{50}$  values of 17.7  $\mu$ M, 24.2  $\mu$ M, 14.3  $\mu$ M, and 55.2  $\mu$ M for albendazole, albendazole  
294 sulfoxide, mebendazole and oxfendazole, respectively, indicating that oxfendazole was the least  
295 potent among the four benzimidazoles(26). Correspondingly,  $ED_{50}$  (dose at 50% worm burden

reduction) values of oxfendazole and albendazole were higher than that of mebendazole in *T. muris* infected mice. The ED<sub>50</sub> values obtained were: Oxfendazole >300 mg/kg, albendazole = 345 mg/kg and mebendazole = 79 mg/kg(26). The study author speculated that oxfendazole would not be any better than albendazole and mebendazole in treating whipworm infection in humans. However, this conclusion may be premature based on the following two considerations: First, the exposure of oxfendazole in human was 27 times higher than that of albendazole sulfoxide (the major active moiety in human plasma following albendazole oral administration) and 538 times higher than that of mebendazole (23-25). Meanwhile, the oxfendazole IC<sub>50</sub> determined *in vitro* was higher than that of albendazole sulfoxide and mebendazole by only 2-4 fold(26). Thus, the higher exposure of oxfendazole compared to albendazole sulfoxide and mebendazole could potentially compensate for oxfendazole lower *in vitro* potency. Second, mice might not be a good model for oxfendazole disposition and efficacy in human due to potentially different pharmacokinetic features. Oxfendazole's metabolic profile in mice is not currently available. However, according to oxfendazole pharmacokinetic studies in the rat, following oxfendazole oral administration, oxfendazole sulfone was the most abundant moiety in plasma followed by oxfendazole and fenbendazole(27). Meanwhile, in humans, oxfendazole was the predominant moiety in plasma followed by oxfendazole sulfone and fenbendazole(21). Considering that oxfendazole and fenbendazole are active while oxfendazole sulfone is inactive, the lack of efficacy in mice might be due to oxfendazole pharmacokinetics (i.e., low systemic exposure) rather than pharmacodynamics (i.e., *in vitro* IC<sub>50</sub>).

It is worth pointing out that the current model was developed based on oxfendazole pharmacokinetics and safety data obtained from healthy adults. When oxfendazole is to be used in patients with neglected tropical infections in Sub-Saharan Africa, South-East Asia and South

319 America, some differences in subjects' physical and health status might affect oxfendazole's  
320 exposure and response. For example, subjects in our study are primarily Caucasian with an  
321 average weight of 82.4 kg, which is 32-55% higher than the average weight of adults in Africa  
322 and South-East Asia(28). Another difference is with baseline hemoglobin concentrations.  
323 Patients in neglected tropical disease pandemic area might have low baseline hemoglobin  
324 concentrations due to other conditions, such as malaria(29) or hookworm infection(30). In our  
325 study, oxfendazole appeared to have a mild suppressive effect on hemoglobin concentrations,  
326 therefore, attention to hemoglobin concentrations in future studies in patients are warranted.

327 In conclusion, we have developed a robust popPK/PD model which can adequately characterize  
328 oxfendazole pharmacokinetics and its effect on hemoglobin concentration in healthy adults  
329 following multiple ascending doses (3 – 15 mg/kg), and the effect of food on oxfendazole  
330 pharmacokinetics. The model was used to comprehensively evaluate the probability of target  
331 attainment of oxfendazole for whipworm infection and filariasis in human following various  
332 dose regimens and under different target attainment criteria. Due to the lack of available data on  
333 oxfendazole exposure-response in against whipworm infection in human, results of target  
334 attainment analysis should be interpreted with caution. Nevertheless, the results of our modeling  
335 work, especially the target attainment analysis, are valuable for dose regimen selection in future  
336 trials in patient populations with different types of parasitic infections.

337



338 **4 METHODS**

339 **4.1 Clinical data**

340 The data used for popPK/PD model development comes from the multiple ascending dose and  
341 food-effect study of oxfendazole in healthy adults that was published recently(23). Key  
342 information of the study is summarized below.

343 The study enrolled 36 subjects, 24 subjects in the multiple ascending dose evaluation and 11  
344 subjects in the food-effect evaluation. Subject demographics are summarized in **Supplementary**  
345 **Table S1**. Overall, demographic and baseline characteristics were similar across dose groups and  
346 dosing conditions. In the multiple ascending dose evaluation, subjects were randomized into  
347 three groups (8 subjects /group) corresponding to oxfendazole doses of 3, 7.5, and 15 mg/kg.  
348 Oxfendazole was administered as an oral suspension in a fasted state once daily for 5 days.  
349 Blood samples for pharmacokinetics assessment were collected on Day 1 at pre-dose and at 0.5,  
350 1, 2, 3, 4, 6, 9, and 12 h post-dose. On Day 2, 3 and 4, samples were collected pre-dose and at 2 h  
351 post-dose. Samples were collected at 0, 0.5, 1, 2, 3, 4, 6, 9, 12, 24, 72 and 120 h after the last  
352 dose. Blood samples for safety assessment including hematology, biochemistry, and coagulation  
353 studies were collected at pre-dose on Day 1, 3, and 5, and at 72 h and 120 h after the last dose.

354 The food-effect evaluation adopted a randomized two-period (separated by 7 days) cross-over  
355 study design with subjects taking a single oral dose of oxfendazole at 3 mg/kg following an  
356 overnight fast or a high-fat breakfast. Blood samples for oxfendazole quantification were  
357 collected at pre-dose and at 0.5, 1, 2, 3, 4, 5, 6, 9, 12, and 24 h after each dose and one sample  
358 was collected from each subject on Day 14. For safety assessment, blood samples were collected  
359 at pre-dose, Day 4, and Day 14.

360 The oxfendazole concentration in plasma was quantified using a validated liquid  
361 chromatography-tandem mass spectrometry assay with linear range of 0.5 – 1000 ng/mL(31).  
362 Intra-day and inter-day accuracy of the quantitative method was in the range of 106.9 – 109.5%,  
363 and the coefficient of variability was no greater than 13.6%(31). Samples above the upper limit  
364 of quantification were diluted appropriately with blank human plasma(31). All samples were  
365 analyzed within the previously established stability time frame.

366 In total, 648 and 252 pharmacokinetics samples were collected and analyzed for the multiple  
367 ascending dose evaluation and the food-effect evaluation, respectively. Seven samples were  
368 disregarded due to sample misidentification. One hundred and twenty samples from the multiple  
369 ascending dose study and 36 samples from the food-effect study were collected and analyzed for  
370 safety assessment. There was no drug-related change in any of the safety parameters except for  
371 hemoglobin concentrations in subjects in the multiple ascending dose study(23). Therefore, only  
372 hemoglobin concentrations from subjects in the multiple ascending dose evaluation were  
373 included in the popPK/PD model.

374 **4.2 Population pharmacokinetic-pharmacodynamic development**

375 NONMEM 7.4.0 (Icon Development, Ellicott City, MD, USA) with stochastic approximation  
376 expectation-maximization (SAEM) method and ADVAN13 subroutine was employed for  
377 nonlinear mixed-effect modeling. Visual predictive checks were performed using Perl-speaks-  
378 NONMEM (PsN) 4.8.0 (Uppsala Pharmacometrics Group) interfaced with Pirana 2.9.9 (Certara,  
379 Princeton, NJ, USA). R 4.0.2 (R Core Team) and RStudio 1.4.1103 (RStudio, PBC, Boston, MA,  
380 USA) were used for data processing and visualization.

#### 381 4.2.1 Handling of missing and BLQ data

382 Less than 2% clinical samples (14 out of 893 samples) had a concentration below the limit of  
383 quantification (BLQ). Because the number of BLQ samples was low and all BLQ samples were  
384 collected after 120 h (i.e., more than 5 half-lives of oxfendazole), BLQ data were omitted from  
385 the popPK/PD analysis.

#### 386 4.2.2 Structural model

387 Structural pharmacokinetic and pharmacodynamic models were developed sequentially.

388 Pharmacokinetic model: The structural pharmacokinetic model for oxfendazole and metabolites  
389 in healthy adults following the administration of single ascending doses published previously(32)  
390 was adopted as the starting model. This model consisted of a depot compartment and a  
391 distribution compartment with first-order absorption and elimination. Because oxfendazole is a  
392 BCS class II drug with low solubility, the drug's bioavailability decreases with increasing dose,  
393 which resulted in a less-than-dose proportional increase in exposure following ascending doses.  
394 Additionally, when oxfendazole was administered following a high fat meal, the bioavailability  
395 was increased. Consequently, oxfendazole bioavailability ( $F$ ) was modeling using the following  
396 equation,

397

$$398 \log(F) = \theta_1 \log\left(\frac{Dose}{\theta_2}\right) + (fast - 1)\log(\theta_3) \quad (1)$$

399 Where  $fast = 0$  if oxfendazole is administered in the fasted state, otherwise  $fast = 1$ .

400 According to equation (1), in the fasted state

$$401 \log(F_{fast}) = \theta_1 \log\left(\frac{Dose}{\theta_2}\right) - \log(\theta_3) \quad (2)$$

402 And in the fed state

$$403 \quad \log(F_{fed}) = \theta_1 \log\left(\frac{Dose}{\theta_2}\right) \quad (3)$$

404 Therefore

$$405 \quad \log\left(\frac{F_{fed}}{F_{fast}}\right) = \log(F_{fed}) - \log(F_{fast}) = \log(\theta_3) \quad (4)$$

406 Thus

$$407 \quad \theta_3 = \frac{F_{fed}}{F_{fast}} \quad (5)$$

408 To simplify parameter estimation, it was assumed that  $F = 1$  at the lowest dose in the fed state.

409 Thus,  $\theta_2$  was fixed to 209.25 mg (corresponding to 3 mg/kg dose in a subject weighing 69.8 kg).

410 To capture the prolonged absorption phase of oxfendazole following consumption of a fatty  
411 meal, absorption models with 1 and 2 transit compartments were examined.

412 Pharmacodynamic model: Exploratory analysis was performed by plotting the observed  
413 oxfendazole concentrations versus observed the hemoglobin concentrations (**Supplementary**  
414 **Figure S3**). Based on **Supplementary Figure S3**, no direct relationship was observed between  
415 oxfendazole and hemoglobin concentrations. Because hemoglobin concentrations were lower  
416 following the administration of multiple higher oxfendazole doses, indirect response models with  
417 either inhibition of hemoglobin synthesis or stimulation of hemoglobin elimination are plausible.  
418 Since oxfendazole inhibits tubulin assembly(33), oxfendazole has suppressive effect on  
419 progenitor cells undergoing extensive cell division in the bone marrow, making more likely  
420 indirect response models with oxfendazole reducing hemoglobin synthesis. Two indirect

response models of the inhibition of hemoglobin synthesis were evaluated: the basic indirect response model and the lifespan indirect response model incorporating red blood cell lifespan. In the basic indirect response model, the change in hemoglobin concentration ( $C_{Hb}$ ) was modeled using the equation

$$\frac{dC_{Hb}}{dt} = k_{in}f(C_{OxF}(t)) - k_{out}C_{OxF} \quad (6)$$

Where  $k_{in}$  is the red blood cell synthesis rate constant and  $k_{out}$  is the red blood cell elimination rate constant.

The change in hemoglobin concentration ( $C_{Hb}$ ) in the lifespan model was modeled as follows,

$$\frac{dC_{Hb}}{dt} = k_{in}f(C_{OxF}(t)) - k_{in}f(C_{OxF}(t - T_R)) \quad (7)$$

Where  $T_R$  represents red blood cell lifespan,  $f(C_{OxF}(t))$  is a function reflecting the inhibitory effect of oxfendazole concentration in the body at time  $t$  ( $C_{OxF}(t)$ ). Linear and nonlinear correlations between oxfendazole concentration and oxfendazole inhibitory effect was evaluated. For linear correlation,

$$f(C_{OxF}(t)) = 1 - \theta \cdot C_{OxF}(t) \quad (8)$$

$$f(C_{OxF}(t - T_R)) = 1 - \theta \cdot C_{OxF}(t - T_R) \quad (9)$$

For nonlinear correlation,

$$f(C_{OxF}(t)) = 1 - \frac{I_{max}C_{OxF}(t)}{IC_{50} + C_{OxF}(t)} \quad (10)$$

$$f(C_{OxF}(t - T_R)) = 1 - \frac{I_{max}C_{OxF}(t - T_R)}{IC_{50} + C_{OxF}(t - T_R)} \quad (11)$$

Where  $I_{max}$  is the maximal inhibitory effect,  $IC_{50}$  is oxfendazole concentration at 50% inhibition,  $C_{OXF}(t)$  is oxfendazole concentration in the body at time  $t$ , and  $C_{OXF}(t - T_R)$  is oxfendazole concentration in the body at time  $t - T_R$ .

#### 4.2.3 Stochastic model

Inter-individual variability and inter-occasion variability were evaluated using the exponential model.

$$P_i = TVP \cdot \exp(\eta_{i,0} + OCC_1 \cdot \eta_{i,1} + OCC_2 \cdot \eta_{i,2}) \quad (5)$$

Where  $TVP$  represents the population mean of a pharmacokinetics or pharmacodynamic parameter,  $P_i$  represents the individual estimate of the corresponding parameter,  $\eta_{i,0}$  represents inter-individual variability,  $\eta_{i,1}$  and  $\eta_{i,2}$  are inter-occasion variabilities following the first and last doses.  $OCC_1 = 1$  for the first dose, otherwise  $OCC_1 = 0$ .  $OCC_2 = 1$  for the last dose, otherwise  $OCC_2 = 0$ . Inter-individual variability and inter-occasion variability are assumed to have a normal distribution with mean 0 and variance  $\omega_{IV}^2$  and  $\omega_{OV}^2$ , respectively.

For residual variability, an additive error model, a proportional error model, and a combined additive and proportional error model were examined. The following is an example of the combined additive and proportional error model.

$$C_{ij} = \overline{C}_{ij} \cdot (1 + \epsilon_{1ij}) + \epsilon_{2ij} \quad (6)$$

$C_{ij}$  is the observed concentrations for individual  $i$  at time  $j$ ,  $\overline{C}_{ij}$  is the corresponding model predicted concentration, and  $\epsilon_{1ij}$  and  $\epsilon_{2ij}$  are proportional and additive errors, respectively. Additive and proportional residual variabilities were assumed to be normally distributed around 0 with variance of  $\sigma_1^2$  and  $\sigma_2^2$ , respectively.

#### 4.2.4 Covariate model

Initially, clinically meaningful covariates including sex, age, weight, BMI, and creatinine clearance were plotted against inter-individual variability of each pharmacokinetic and pharmacodynamic parameter. Potential covariates identified through graphical analysis were examined using stepwise forward addition and backward elimination. For stepwise forward addition, a decrease in objective function value (OFV) of more than 6.63 (p-value < 0.01) was considered significant improvement in model performance. For stepwise backward elimination, an increase in OFV of more than 10.83 (p-value < 0.001) was considered significant deterioration in model performance. The effect of continuous variables (i.e., age, weight, BMI, and creatinine clearance) were evaluated using the following general equation,

$$TVP_i = TVP \left( \frac{cov_i}{cov_m} \right)^{\theta_{cov}} \quad (7)$$

Where  $TVP_i$  is the individual PK/PD parameter,  $TVP$  is the population mean of the corresponding PK/PD parameter,  $cov_i$  is the individual covariate,  $cov_m$  is the population mean of the covariate, and  $\theta_{cov}$  is the covariate effect.

The effect of sex, a categorical variable, was assessed using the equation,

$$TVP_i = TVP_{male} \cdot (\theta_{sex})^{Sex} \quad (8)$$

Where  $TVP_{male}$  is the value of the PK/PD parameter in males.  $Sex = 1$  for females and 0 for males. Thus,  $\theta_{sex}$  is the ratio of a PK/PD parameter in females over that in males.

#### 4.2.5 Model evaluation

Models were selected based on feasibility and precision of parameter estimates and goodness-of-fit plots including the plots of i) observed concentration versus population predicted

481 concentration, ii) observed concentration versus individual predicted concentration, iii)  
482 conditional weighted residual (CWRES) versus population predicted concentration, and iv)  
483 CWRES versus time. For a good model, all data points would scatter evenly around the identity  
484 line in the former two plots, and around the zero line in the latter two plots. Nested models were  
485 compared based on the difference in OFV ( $\Delta$ OFV).  $\Delta$ OFV was assumed to have a  $\chi^2$  distribution  
486 with the degree of freedom being the difference in the number of parameters between the two  
487 nested models. On this basis, the addition of one parameter to the model was considered  
488 significantly improved model performance if OFV decreased more than 6.63, corresponding to  
489 p-value < 0.01. For non-nested models, AIC was used. The model with a smaller AIC was  
490 considered better.

491 Model predictive performance was evaluated using prediction-corrected visual predictive check  
492 of 1000 simulations. Model predictive performance was acceptable if the observed 5<sup>th</sup>, 50<sup>th</sup> and  
493 95<sup>th</sup> percentiles fall within the 95% confidence interval of the corresponding simulated  
494 percentiles.

### 495 **4.3 Simulation**

#### 496 **4.3.1 Simulation of exposure-response on safety**

497 The simulation of exposure-response on safety focused on the effect of administration of  
498 multiple ascending doses of oxfendazole at 3, 7.5, 15, 30 and 60 mg/kg once daily for 5 days on  
499 hemoglobin concentrations in healthy adults. A thousand subjects were simulated for each dose  
500 level, assuming 1:1 ratio of female to male subjects. Oxfendazole was administered using  
501 weight-normalized dose, but oxfendazole bioavailability depends on the absolute dose present in  
502 the gastrointestinal tract; therefore, subject weight needs to be included in the simulation to  
503 convert from weight-normalized dose to absolute dose. Subject weight distribution was based on



the observed weight of participants in the oxfendazole multiple ascending dose trial. Female weight was simulated based on a normal distribution of mean 77.4 kg and standard deviation of 14.2 kg. For males, the mean weight was 84.6 kg and standard deviation was 13.0 kg. The simulated hemoglobin concentrations obtained were viewed in light of standard normal sex specific hemoglobin ranges.

#### 4.3.2 Simulation of exposure-response on efficacy

##### Target attainment analysis for whipworm infection – 1<sup>st</sup> approach

Factors determining the effect of oxfendazole on *Trichuris trichiura* (human whipworm) is largely unknown. To carry out target attainment analysis, several assumptions were made based on literature information as provided below.

In a drug disposition study by Hansen et al.(22), a single oral dose of oxfendazole at 5 mg/kg was administered to pigs infected with *T. suis*. Blood samples and large intestinal samples were collected from the pigs over 48 h for quantification of oxfendazole in pig plasma, whole cecal tissue, cecal mucosa, cecal content, and in whipworm. This study found that the concentration of oxfendazole in pig plasma ( $C_{OXF,plasma}$  (nmol/mL)) was closely associated with the concentration of oxfendazole in whipworm ( $C_{OXF,whorm}$  (nmol/g)). Since the porcine parasite *T. suis* and the human infecting *T. trichiura* have very similar growth habits, the anterior of the worm penetrating into the intestinal mucosa, with the posterior of the parasite freely moving in the intestinal lumen(22, 34), the findings of the Hansen study(22) are thought to be relevant also for the human *T. trichiura* infection. Further, the relative exposure to oxfendazole and its metabolites (oxfendazole sulfone and fenbendazole) in pigs and in humans is similar(21, 22), suggesting that pig is a good model for oxfendazole disposition in human. Thus, the correlation

526 between oxfendazole concentration in host plasma and in intestinal dwelling whipworm was  
527 assumed to be similar for humans and pigs.

528 We digitized the data reported by Hansen et al.(22) using Engauge Digitizer(35), and converted  
529 oxfendazole concentration in whipworm in nmol/g to concentration in nmol/mL based on body  
530 density of nematodes derived using the formulas for nematode body weight and body volume  
531 proposed by Andrassy(36).

$$532 \quad weight(\mu g) = \frac{length(\mu m) \times (diameter(\mu m))^2}{1.6 \times 10^{-6}} \quad (9)$$

$$533 \quad volume(\mu m^3) = \frac{length(\mu m) \times (diameter(\mu m))^2}{1.7} \quad (10)$$

534 According to the above equations, all nematodes have the same body density.

$$535 \quad density = \frac{weight}{volume} = 1.0625 \times 10^{-6} \frac{\mu g}{\mu m^3} \quad (11)$$

536 Based on the digitized data, the ratio between oxfendazole concentration in worm and  
537 oxfendazole concentration in pig plasma was quite consistent over time with the average value of  
538  $C_{OXF,worm}(nmol/mL)/C_{OXF,plasma}(nmol/mL) = 3.29$ .

539 The principle pharmacological activity of benzimidazoles, including oxfendazole, stems from the  
540 their binding to tubulin resulting in inhibition of tubulin assembly(33). Oxfendazole IC<sub>50</sub> (drug  
541 concentration causing 50% inhibition) to *T. trichiura* tubulin is unknown. However, an *in vitro*  
542 experiment evaluating oxfendazole inhibitory effect on tubulin extracted from *Ascaris galli*  
543 (roundworm in bird) reported an IC<sub>50</sub> of 5 μM (~1580 ng/mL)(37). Because *A. galli* and *T.*  
544 *trichiura* are both intestinal nematodes, it was speculated that oxfendazole IC<sub>50</sub> to *T. trichiura*  
545 tubulin and *A. galli* tubulin would be similar.

To summarize, *in vitro* and preclinical efficacy data were applied to target attainment analysis for the treatment of whipworm infection in human based on the following assumptions:

- Assumption 1:  $C_{OXF,worm}(nmol/mL)/C_{OXF,plasma}(nmol/mL) = 3.29$ .
- Assumption 2: oxfendazole  $IC_{50}$  to whipworm tubulin and *A. galli* tubulin is the same and is equivalent to 1580 ng/mL.
- Assumption 3: the worm body is a well-stirred model.

Based on the above assumptions, oxfendazole  $IC_{50} = 1580$  ng/mL at the site of tubulin assembly corresponds to oxfendazole concentration of 480 ng/mL in human plasma.

Oxfendazole concentration time profiles were simulated following the administration of multiple ascending oxfendazole doses of 0.5 – 60 mg/kg once daily for 5 days with 1000 subjects at each dose. Subject sex and weight distribution was the same as in the safety simulation. Because it is unknown whether the antiparasitic efficacy of oxfendazole depends on the achievement of an effective concentration or the maintenance over some time period of the effective concentration, two scenarios were investigated. In the first scenario, oxfendazole antiparasitic efficacy was assumed to be dependent on attainment of a targeted  $C_{max,ss}$ . The range of targeted  $C_{max,ss}$  evaluated was 1 – 40 times  $IC_{50}$  (480 ng/mL). In the second scenario, oxfendazole antiparasitic efficacy was assumed to be dependent on maintenance of the oxfendazole concentration above the  $IC_{50}$  for a certain amount of time, as reflected by the percent time dosing interval (24 h) at steady state during which oxfendazole concentration is above  $IC_{50}$  ( $T_{>IC50}$ ). Ranges of  $T_{>IC50}$  explored included <40%, 40-<60%, 60-<80%, 80-<100%, and 100%. The probability of target attainment is the percentage of simulated subjects being able to attain the targeted  $C_{max,ss}$  or  $T_{>IC50}$ .

568 Target attainment analysis for whipworm infection – 2<sup>nd</sup> approach

569 A recent study by Keiser and Haberli evaluated the survival of *Trichuris muris* (whipworm  
570 collected from rodents) in culture in the presence of various antiparasitic drugs(26). Whipworm  
571 survival was assessed based on whipworm motility. This study reported an IC<sub>50</sub> of 55.2 µM  
572 (~17405 ng/mL) for oxfendazole(26). To utilize this information for target attainment analysis,  
573 the following assumptions were made.

574 - Assumption 1:  $C_{OXF,worm}/C_{OXF,plasma} = 3.29$

575 - Assumption 2: Oxfendazole IC<sub>50</sub> is the same for *T. muris* and *T. trichiura*.

576 Based on the above assumptions, oxfendazole IC<sub>50</sub> of 17405 ng/mL to *T. trichiura* was translated  
577 to 5290 ng/mL in human plasma. Two target attainment analysis were carried out, one evaluating  
578 C<sub>max,ss</sub> and the other evaluating T<sub>>IC50</sub> as described in the 1<sup>st</sup> approach.

579 Target attainment analysis for filariasis

580 To evaluate the macrofilaricidal efficacy of oxfendazole, Hubner et al. utilized *Litomosoides*  
581 *sigmodontis* infected mice, a surrogate model for filariasis in human(13). Oxfendazole was  
582 administered to infected mice orally or subcutaneously once daily or twice daily for 1, 5, or 10  
583 days at doses ranging from 1 to 125 mg/kg per day. Macrofilaricidal efficacy was assessed by  
584 adult worm count. The study showed that sterile cure was achieved with an oral dose of 12.5  
585 mg/kg twice daily for 5 days, or subcutaneous dose of 25 mg/kg once daily for 5 days(13).

586 Concurrently, oxfendazole pharmacokinetics following the administration of a single  
587 subcutaneous dose of 1 and 25 mg/kg or a single oral dose of 5 or 25 mg/kg was evaluated in a  
588 parallel untreated group of mice(13). Based on their efficacy and pharmacokinetic results,  
589 Hubner et al. suggested that oxfendazole macrofilaricidal efficacy is driven by the maintenance

590 of its MEC in plasma above 100 ng/mL(13). Thus, for target attainment analysis, the percentage  
591 of the simulated population with oxfendazole concentration at steady state being  $\geq$  MEC was  
592 computed. To account for the uncertainty extrapolating data from mice to humans, a range of  
593 MEC from 100 to 4000 ng/mL was investigated in the present study.

594

595 **Acknowledgements:** This work was supported by the Division of Microbiology and Infectious  
596 Diseases, National Institute of Allergy and Infectious Diseases, National Institutes of Health  
597 through the Vaccine and Treatment Evaluation Unit (contracts no. HHSN272200800008C and  
598 HHSN24220130020I) and by the National Center for Advancing Translational Sciences grant to  
599 the University of Iowa (grant no. 5U54TR001356) for the work done in the Clinical Research  
600 Unit.

601

602

## 603 REFERENCES

- 604 1. WHO. 2020. Ending the neglect to attain the Sustainable Development Goals - A  
605 roadmap for the neglected tropical diseases 2021-2030.  
606 [https://www.who.int/neglected\\_diseases/Ending-the-neglect-to-attain-the-SDGs--NTD-](https://www.who.int/neglected_diseases/Ending-the-neglect-to-attain-the-SDGs--NTD-Roadmap.pdf)  
607 [Roadmap.pdf](https://www.who.int/neglected_diseases/Ending-the-neglect-to-attain-the-SDGs--NTD-Roadmap.pdf). Accessed February 02, 2021.
- 608 2. Garcia HH, Gilman RH, Horton J, Martinez M, Herrera G, Altamirano J, Cuba JM, Rios-  
609 Saavedra N, Verastegui M, Boero J, Gonzalez AE. 1997. Albendazole therapy for  
610 neurocysticercosis: a prospective double-blind trial comparing 7 versus 14 days of  
611 treatment. *Cysticercosis Working Group in Peru. Neurology* 48:1421-7.
- 612 3. Moser W, Schindler C, Keiser J. 2017. Efficacy of recommended drugs against soil  
613 transmitted helminths: systematic review and network meta-analysis. *BMJ* 358:j4307.
- 614 4. Mihmanli M, Idiz UO, Kaya C, Demir U, Bostanci O, Omeroglu S, Bozkurt E. 2016.  
615 Current status of diagnosis and treatment of hepatic echinococcosis. *World J Hepatol*  
616 8:1169-1181.
- 617 5. Katiyar D, Singh LK. 2011. Filariasis: Current status, treatment and recent advances in  
618 drug development. *Curr Med Chem* 18:2174-85.
- 619 6. Caravedo MA, Cabada MM. 2020. Human fascioliasis: current epidemiological status  
620 and strategies for diagnosis, treatment, and control. *Res Rep Trop Med* 11:149-158.
- 621 7. Dawson M, Allan RJ, Watson TR. 1982. The pharmacokinetics and bioavailability of  
622 mebendazole in man: a pilot study using [3H]-mebendazole. *Br J Clin Pharmacol* 14:453-  
623 5.
- 624 8. Dawson M, Braithwaite PA, Roberts MS, Watson TR. 1985. The pharmacokinetics and  
625 bioavailability of a tracer dose of [3H]-mebendazole in man. *Br J Clin Pharmacol* 19:79-  
626 86.
- 627 9. Corti N, Heck A, Rentsch K, Zingg W, Jetter A, Stieger B, Pauli-Magnus C. 2009. Effect  
628 of ritonavir on the pharmacokinetics of the benzimidazoles albendazole and  
629 mebendazole: an interaction study in healthy volunteers. *Eur J Clin Pharmacol* 65:999-  
630 1006.
- 631 10. Anonymous. 1990. Freedom of Information Summary, NADA 140-854 Synanthic-  
632 original approval.  
633 <https://animaldrugsatfda.fda.gov/adafda/app/search/public/document/downloadFoi/505>.
- 634 11. Alvarez L, Saumell C, Fuse L, Moreno L, Ceballos L, Domingue G, Donadeu M, Dungu  
635 B, Lanusse C. 2013. Efficacy of a single high oxfendazole dose against gastrointestinal  
636 nematodes in naturally infected pigs. *Vet Parasitol* 194:70-4.
- 637 12. Corwin RM, Kennedy JA, Pratt SE. 1979. Dose titration of oxfendazole against common  
638 nematodes of swine. *Am J Vet Res* 40:297-8.
- 639 13. Hubner MP, Martin C, Specht S, Koschel M, Dubben B, Frohberger SJ, Ehrens A,  
640 Fendler M, Struever D, Mitre E, Vallarino-Lhermitte N, Gokool S, Lustigman S,  
641 Schneider M, Townson S, Hoerauf A, Scandale I. 2020. Oxfendazole mediates  
642 macrofilaricidal efficacy against the filarial nematode *Litomosoides sigmodontis* in vivo  
643 and inhibits *Onchocerca* spec. motility in vitro. *PLoS Negl Trop Dis* 14:e0008427.
- 644 14. Gonzalez AE, Codd EE, Horton J, Garcia HH, Gilman RH. 2019. Oxfendazole: a  
645 promising agent for the treatment and control of helminth infections in humans. *Expert*  
646 *Rev Anti Infect Ther* 17:51-56.

- 647 15. Codd EE, Ng HH, McFarlane C, Riccio ES, Doppalapudi R, Mirsalis JC, Horton RJ,  
648 Gonzalez AE, Garcia HH, Gilman RH, Cysticercosis Working Group in P. 2015.  
649 Preclinical studies on the pharmacokinetics, safety, and toxicology of oxfendazole:  
650 toward first in human studies. *Int J Toxicol* 34:129-37.
- 651 16. Gokbulut C, Bilgili A, Hanedan B, McKellar QA. 2007. Comparative plasma disposition  
652 of fenbendazole, oxfendazole and albendazole in dogs. *Vet Parasitol* 148:279-87.
- 653 17. Lanusse CE, Gascon LH, Prichard RK. 1995. Comparative plasma disposition kinetics of  
654 albendazole, fenbendazole, oxfendazole and their metabolites in adult sheep. *J Vet*  
655 *Pharmacol Ther* 18:196-203.
- 656 18. Moreno L, Lopez-Urbina MT, Farias C, Domingue G, Donadeu M, Dungu B, Garcia HH,  
657 Gomez-Puerta LA, Lanusse C, Gonzalez AE. 2012. A high oxfendazole dose to control  
658 porcine cysticercosis: pharmacokinetics and tissue residue profiles. *Food Chem Toxicol*  
659 50:3819-25.
- 660 19. Alvarez LI, Saumell CA, Sanchez SF, Lanusse CE. 1996. Plasma disposition kinetics of  
661 albendazole metabolites in pigs fed different diets. *Res Vet Sci* 60:152-6.
- 662 20. Allan RJ, Watson TR. 1983. The metabolic and pharmacokinetic disposition of  
663 mebendazole in the rat. *Eur J Drug Metab Pharmacokinet* 8:373-81.
- 664 21. An G, Murry DJ, Gajurel K, Bach T, Deye G, Stebounova LV, Codd EE, Horton J,  
665 Gonzalez AE, Garcia HH, Ince D, Hodgson-Zingman D, Nomicos EYH, Conrad T,  
666 Kennedy J, Jones W, Gilman RH, Winokur P. 2019. Pharmacokinetics, safety, and  
667 tolerability of oxfendazole in healthy volunteers: a randomized, placebo-controlled first-  
668 in-human single-dose escalation study. *Antimicrob Agents Chemother*  
669 doi:10.1128/AAC.02255-18.
- 670 22. Hansen TVA, Williams AR, Denwood M, Nejsun P, Thamsborg SM, Friis C. 2017.  
671 Pathway of oxfendazole from the host into the worm: *Trichuris suis* in pigs. *International*  
672 *Journal for Parasitology-Drugs and Drug Resistance* 7:416-424.
- 673 23. Bach T, Galbiati S, Kennedy JK, Deye G, Nomicos EYH, Codd EE, Garcia HH, Horton  
674 J, Gilman RH, Gonzalez AE, Winokur P, An G. 2020. Pharmacokinetics, Safety, and  
675 Tolerability of Oxfendazole in Healthy Adults in an Open Label Phase 1 Multiple  
676 Ascending Dose and Food Effect Study. *Antimicrob Agents Chemother*  
677 doi:10.1128/AAC.01018-20.
- 678 24. Lange H, Eggers R, Bircher J. 1988. Increased systemic availability of albendazole when  
679 taken with a fatty meal. *Eur J Clin Pharmacol* 34:315-7.
- 680 25. Janssen. June 2017 2017. Mebendazole label, on Janssen.  
681 [https://www.accessdata.fda.gov/drugsatfda\\_docs/label/2016/208398s000lbl.pdf](https://www.accessdata.fda.gov/drugsatfda_docs/label/2016/208398s000lbl.pdf).  
682 Accessed January 26, 219.
- 683 26. Keiser J, Haberli C. 2021. Evaluation of Commercially Available Anthelmintics in  
684 Laboratory Models of Human Intestinal Nematode Infections. *ACS Infect Dis*  
685 doi:10.1021/acsinfecdis.0c00719.
- 686 27. FAO. 1998. Residues of some veterinary drugs in foods and animals: 41-4-oxfendazole.  
687 [http://www.fao.org/fileadmin/user\\_upload/vetdrug/docs/41-4-oxfendazole.pdf](http://www.fao.org/fileadmin/user_upload/vetdrug/docs/41-4-oxfendazole.pdf). Accessed  
688 28. Hayes DJ, Buuren Sv, Ter Kuile FO, Stasinopoulos DM, Rigby RA, Terlouw DJ. 2014.  
689 Developing regional weight-for-age growth references for malaria-endemic countries to  
690 optimize age-based dosing of antimalarials. *Bulletin of the World Health organization*  
691 93:74-83.
- 692 29. White NJ. 2018. Anaemia and malaria. *Malar J* 17:371.



- 693 30. Layrisse M, Roche M. 1964. The relationship between anemia and hookworm infection.  
694 Results of surveys of rural Venezuelan population. *Am J Hyg* 79:279-301.
- 695 31. Bach T, Bae S, D'Cunha R, Winokur P, An G. 2019. Development and validation of a  
696 simple, fast, and sensitive LC/MS/MS method for the quantification of oxfendazole in  
697 human plasma and its application to clinical pharmacokinetic study. *J Pharm Biomed*  
698 *Anal* 171:111-117.
- 699 32. Bach T, Murry DJ, Stebounova LV, Deye G, Winokur P, An G. 2021. Population  
700 Pharmacokinetic Model of Oxfendazole and Metabolites in Healthy Adults following  
701 Single Ascending Doses. *Antimicrob Agents Chemother* doi:10.1128/AAC.02129-20.
- 702 33. McKellar QA, Scott EW. 1990. The benzimidazole anthelmintic agents--a review. *J Vet*  
703 *Pharmacol Ther* 13:223-47.
- 704 34. CDC. Trichuriasis. <https://www.cdc.gov/parasites/whipworm/biology.html>. Accessed 06  
705 April 2021.
- 706 35. Mitchell M, Muftakhidinov B, Winchen T, Wilms A, Schaik Bv, Mo-Gul b, Badger TG,  
707 Jędrzejewski-Szmek Z, Kensington, Kylesower. Engauge Digitizer Software.  
708 <https://markummitchell.github.io/engauge-digitizer/>. Accessed 06-29-2021.
- 709 36. Andrassy I. 1956. Die rauminhalts-und gewichtsbestimmung der fadenwürmer  
710 (Nematoden). *Acta Zoologica Hungarica* 2:1-5.
- 711 37. Dawson PJ, Gutteridge WE, Gull K. 1984. A comparison of the interaction of  
712 anthelmintic benzimidazoles with tubulin isolated from mammalian tissue and the  
713 parasitic nematode *Ascaridia galli*. *Biochem Pharmacol* 33:1069-74.
- 714

715 **LIST OF FIGURES**

716 **Figure 1.** A) Structural PK/PD model for oxfendazole and its effect on hemoglobin  
717 concentration following multiple ascending doses and following single dose in the fasted state.

718 B) Structural PK model for oxfendazole following single oral dose in the fed state.

719 **Figure 2.** Time course of population predicted oxfendazole concentration and observed  
720 oxfendazole concentration following multiple ascending doses at 3, 7.5 and 15 mg/kg once daily  
721 for 5 days (upper panel) and following a single 3 mg/kg dose in fasted state and fed state (lower  
722 panel). Observed concentrations are presented as mean  $\pm$  standard deviation for each group (N =  
723 8 for multiple ascending doses evaluation, N = 12 for food effect evaluation).

724 **Figure 3.** Time course of the change in population predicted hemoglobin concentration and  
725 change in observed hemoglobin concentration from baseline following multiple ascending doses  
726 at 3, 7.5 and 15 mg/kg once daily for 5 days. Observed concentrations are presented as mean  $\pm$   
727 standard deviation for each dose group (N = 8).

728 **Figure 4.** Prediction-corrected visual predictive check for A) oxfendazole concentration in  
729 plasma following multiple ascending doses (3 – 15 mg/kg once daily for 5 days), B) hemoglobin  
730 concentration in plasma following multiple ascending doses, C) oxfendazole concentration in  
731 plasma following a single 3 mg/kg dose in fasted state, and D) oxfendazole concentration in  
732 plasma following a single 3 mg/kg dose in fed state.

733 **Figure 5.** Simulated hemoglobin concentration in male and female subjects administered 3, 7.5,  
734 15, 30, and 60 mg/kg oxfendazole once daily for 5 days.

735 **Figure 6.** Probability of target attainment for whipworm infection following multiple ascending  
736 doses of oxfendazole (0.5 – 60 mg/kg once daily for 5 days) – 1<sup>st</sup> approach. Probability of target

737 attainment is the percentage of simulated subjects (1000 subjects at each dose level) having

738 plasma oxfendazole  $C_{\max,ss} = 1 - 40 IC_{50}$ .  $IC_{50} = 480$  ng/mL.

739 **Figure 7.** Probability of target attainment for whipworm infection following multiple ascending

740 doses of oxfendazole (0.5 – 60 mg/kg once daily for 5 days) – 2<sup>nd</sup> approach. Probability of target

741 attainment is the percentage of simulated subjects (1000 subjects at each dose level) having

742 plasma oxfendazole  $C_{\max,ss} = 1 - 5 IC_{50}$ .  $IC_{50} = 5290$  ng/mL.

743 **Figure 8.** A) Mean simulated concentration-time profile of oxfendazole in human plasma

744 following multiple ascending doses of oxfendazole 0.5-60 mg/kg once daily for 5 days compared

745 to different minimal efficacious concentrations (MEC) of 100 – 4000 ng/mL B) Probability of

746 target attainment for filariasis following multiple ascending doses of oxfendazole (0.5 – 60

747 mg/kg once daily for 5 days). Probability of target attainment is the percentage of simulated

748 subjects (1000 subjects at each dose level) having plasma oxfendazole concentration at steady

749 state above MEC for 100% of the dosing interval (i.e., 24 h).

750

751

752 **Table 1.** Final estimates of oxfendazole population pharmacokinetic-pharmacodynamic model  
753 parameters.

Parameter	Definition	Estimate	%RSE <sup>b</sup>	%Shrinkage
$\theta_1$	A parameter in calculation of bioavailability (F) <sup>a</sup>	-0.646	11.2	
$\theta_2$ (mg)	A parameter in calculation of bioavailability (F) <sup>a</sup>	209.25 FIX		
$F_{\text{fed}}/F_{\text{fast}}$	Ratio of bioavailability in fed state to bioavailability in fasted state	2.08	12.4	
$k_{\text{TR}}$ (h <sup>-1</sup> )	First-order transit rate constant in fed state	0.412	14.7	
$k_a$ (h <sup>-1</sup> )	First-order absorption rate constant in fasted state	1.2	7.1	
$V_{\text{OXF}}$ (L)	Oxfendazole apparent volume of distribution	34.5	8.0	
$CL_{\text{OXF}}$ (L/h)	Oxfendazole apparent clearance	2.57	8.6	
$\theta$ (mL/ng)	Linear coefficient for the inhibitory effect of oxfendazole on hemoglobin synthesis	0.000458	9.5	
$k_{\text{in}}$ (g/dL/h)	Zero-order rate constant of hemoglobin synthesis in male	0.00509	1.6	
$T_R$ (h)	Red blood cell lifespan	2880 FIX		
$\theta_{\text{sex}}$	The ratio of $k_{\text{in}}$ in female to $k_{\text{in}}$ in male	0.913	2.7	
$k_{\text{TR}}$ IIV (CV%)	Inter-individual variability in $k_{\text{TR}}$	47.4	52.0	44
$k_a$ IIV (CV %)	Inter-individual variability in $k_a$	28.6	90.6	31
$V_{\text{OXF}}$ IIV (CV%)	Inter-individual variability in $V_{\text{OXF}}$	20.1	59.9	17
$CL_{\text{OXF}}$ IIV (CV%)	Inter-individual variability in $CL_{\text{OXF}}$	37.3	33.2	7
$\rho_{V_{\text{OXF}}, CL_{\text{OXF}}}$ IIV	Correlation of $V_{\text{OXF}}$ IIV and $CL_{\text{OXF}}$ IIV	0.771	10.9	
$V_{\text{OXF}}$ IOV (CV%)	Inter-occasion variability in $V_{\text{OXF}}$	24.1	34.6	21
$CL_{\text{OXF}}$ IOV (CV%)	Inter-occasion variability in $CL_{\text{OXF}}$	32.1	52.6	26
$\rho_{V_{\text{OXF}}, CL_{\text{OXF}}}$ IOV	Correlation of $V_{\text{OXF}}$ IOV and $CL_{\text{OXF}}$ IOV	0.887	15.2	
$k_{\text{in}}$ IIV (CV%)	Inter-individual variability in $k_{\text{in}}$	60.8	35.8	20
$\sigma_{\text{OXF}, \text{prop}}^2$	Variance of oxfendazole proportional residual error	0.0616	10.4	13
$\sigma_{\text{OXF}, \text{add}}^2$	Variance of oxfendazole additive residual error	0.261	69.0	13
$\sigma_{\text{Hb}, \text{prop}}^2$	Variance of hemoglobin proportional residual error	0.000600	14.4	10

754 <sup>a</sup> $\log(F) = \theta_1 \log(\text{Dose}/\theta_2) + (\text{fast}-1) \log(F_{\text{fed}}/F_{\text{fast}})$ , fast = 0 in fasted state, fast = 1 in fed  
755 state.

756 <sup>b</sup>Relative standard error %RSE = standard error  $\times$  100%/parameter estimate

757

758 **Table 2.** Probability of target attainment (%) for whipworm infection following multiple  
 759 ascending doses of oxfendazole (0.5 – 60 mg/kg once daily for 5 days) – 1<sup>st</sup> approach.  
 760 Probability of target attainment is the percentage of simulated subjects (1000 subjects at each  
 761 dose level) having plasma oxfendazole concentration above IC<sub>50</sub> for a certain amount of time.  
 762 T<sub>>IC<sub>50</sub></sub> is the percent time of a dosing interval at steady state during which oxfendazole  
 763 concentration is above IC<sub>50</sub> (IC<sub>50</sub> = 480 ng/mL).

Dose (mg/kg)	T <sub>&gt;IC<sub>50</sub></sub> (%)				
	100	80 – <100	60 – <80	40 – <60	≤40
0.5	27.6	13.0	17.5	26.0	15.9
1	38.0	16.1	17.5	22.0	6.4
1.5	47.0	16.6	15.7	16.7	4.0
3	59.9	14.1	13.0	11.8	1.2
4	64.3	13.7	10.7	10.3	1.0
5	70.9	11.1	9.8	7.3	0.9
7.5	74.9	11.6	7.9	5.2	0.4
10	79.5	10.0	6.2	3.9	0.4
15	82.9	7.6	5.5	3.6	0.4
20	87.9	5.3	4.0	2.6	0.2
30	90.5	5.0	2.8	1.7	0.0
40	90.6	5.3	3.0	0.9	0.2
50	93.5	3.5	2.0	1.0	0.0
60	92.5	3.9	2.7	0.8	0.1

764

765

766

767 **Table 3.** Probability of target attainment (%) for whipworm infection following multiple  
 768 ascending doses of oxfendazole (0.5 – 60 mg/kg once daily for 5 days) – 2<sup>nd</sup> approach.  
 769 Probability of target attainment is the percentage of simulated subjects (1000 subjects at each  
 770 dose level) having plasma oxfendazole concentration above IC<sub>50</sub> for a certain amount of time.  
 771 T<sub>>IC<sub>50</sub></sub> is the percent time of a dosing interval at steady state during which oxfendazole  
 772 concentration is above IC<sub>50</sub> (IC<sub>50</sub> = 5290 ng/mL).

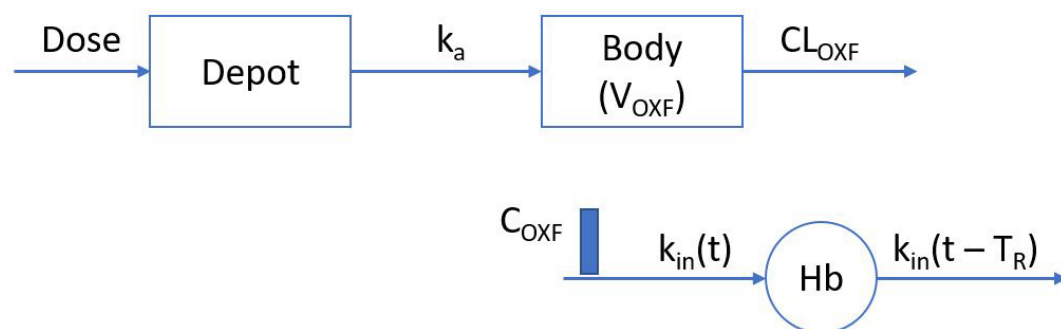
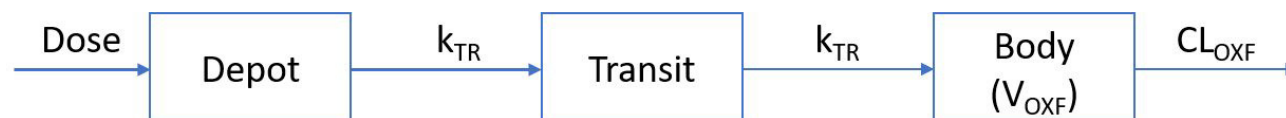
Dose (mg/kg)	T <sub>&gt;IC<sub>50</sub></sub> (%)				
	100	80 – <100	60 – <80	40 – <60	≤40
0.5	0.0	0.0	0.0	0.0	100
1	0.0	0.0	0.0	0.1	99.9
1.5	0.0	0.1	0.1	0.3	99.5
3	0.0	0.0	0.0	0.6	99.4
4	0.0	0.0	0.6	1.2	98.2
5	0.0	0.1	0.2	1.4	98.3
7.5	0.1	0.2	0.8	4.1	94.8
10	0.3	0.9	0.7	4.4	93.7
15	0.5	0.3	2.5	7.0	89.7
20	1.0	1.5	2.3	9.9	85.3
30	1.4	1.7	4.5	15.1	77.3
40	1.8	3.5	5.6	18.1	71.0
50	3.7	4.3	6.7	22.1	63.2
60	4.1	5.0	5.9	22.6	62.4

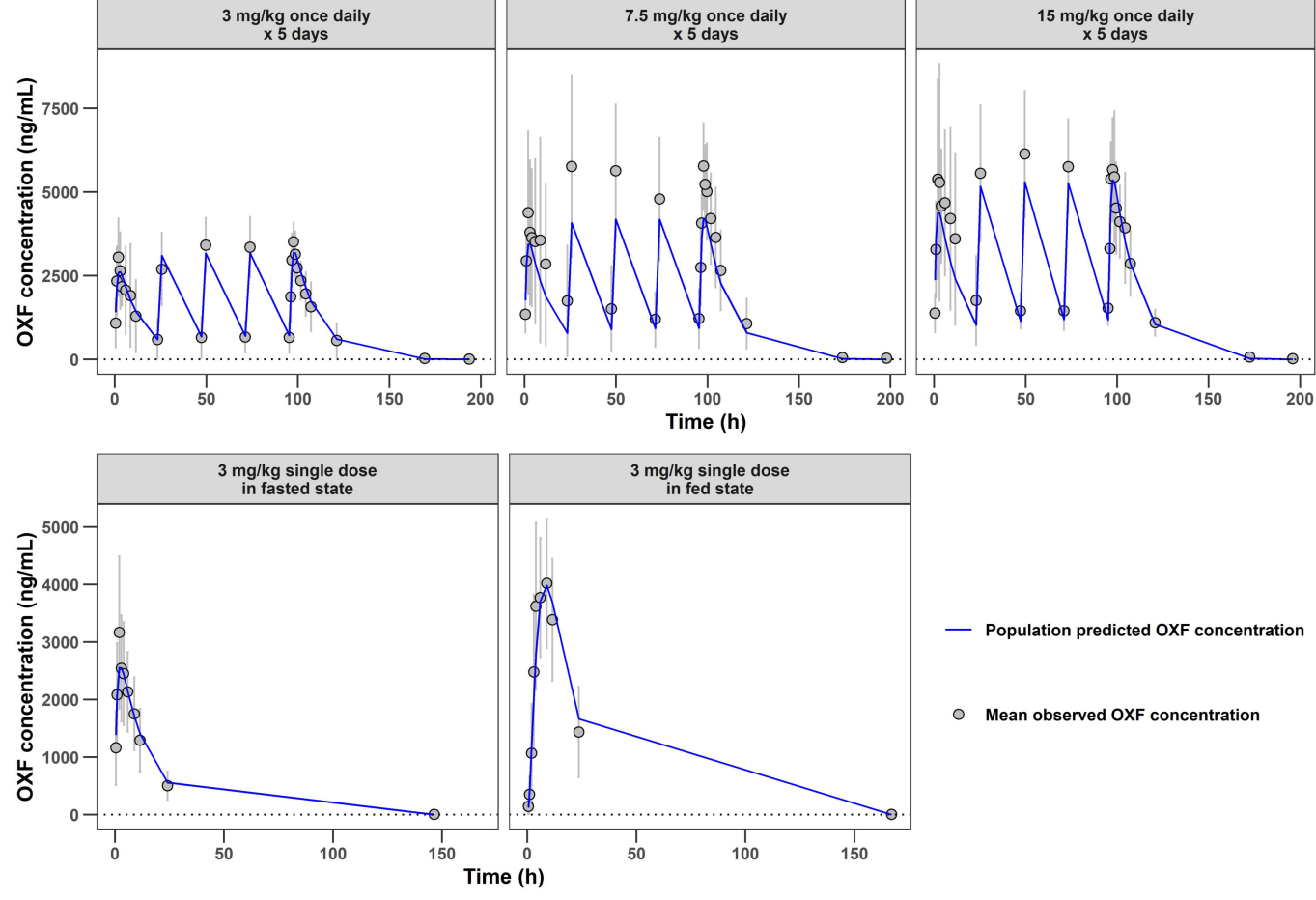
773

774

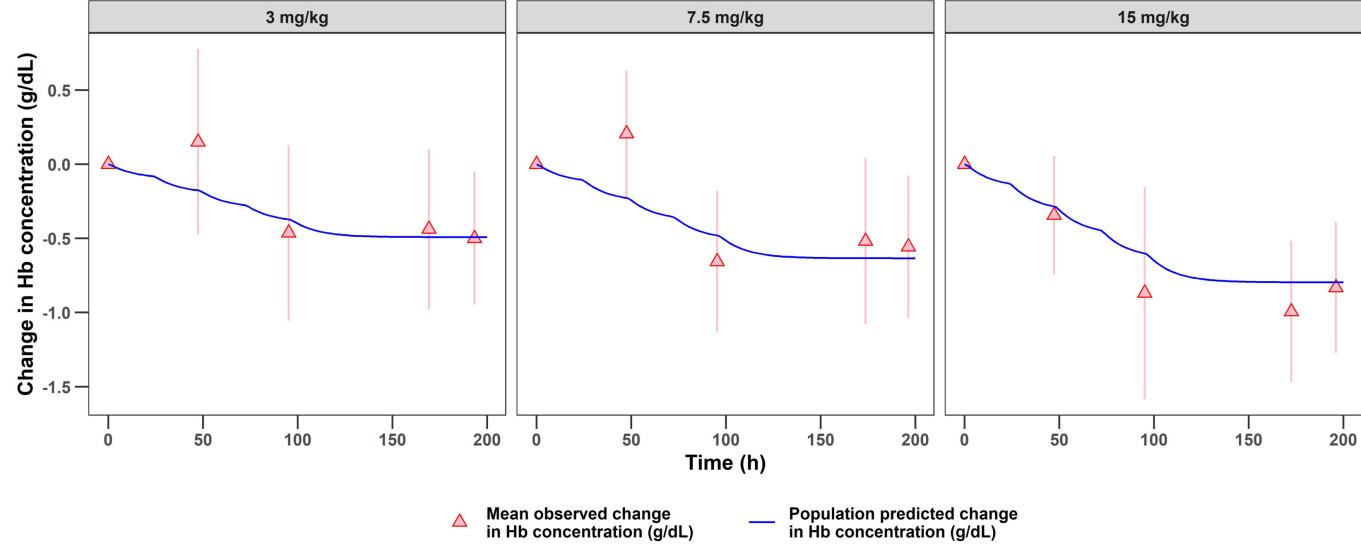
775

776

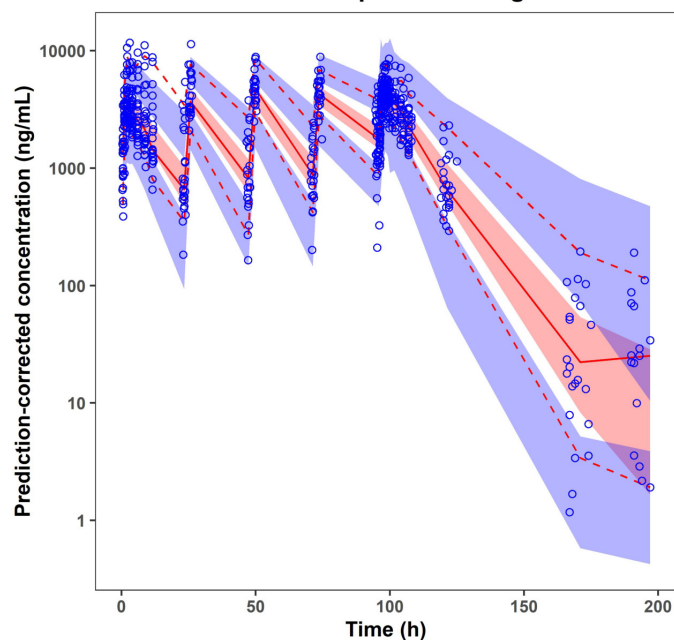
**A. Fasted state****B. Fed state**



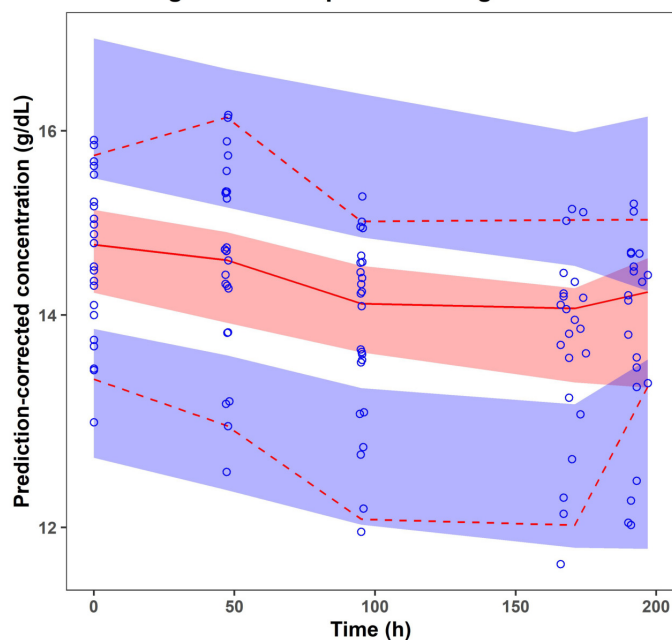




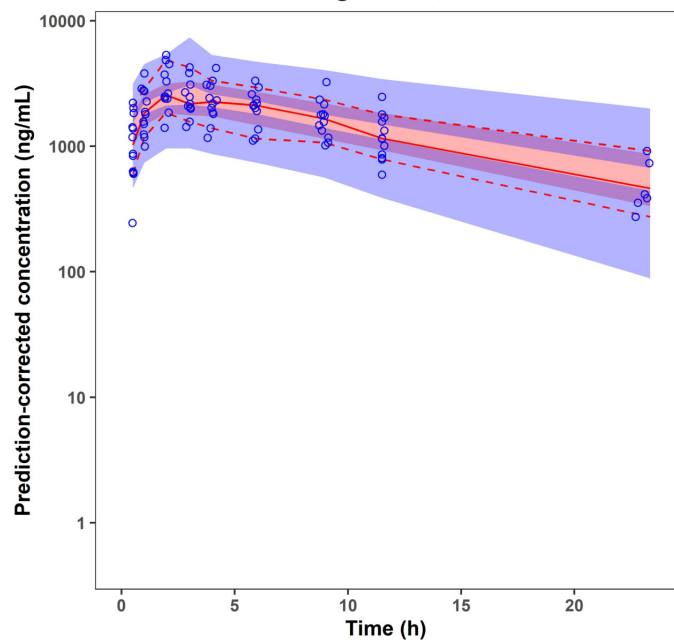
**A. Oxfendazole - multiple ascending dose**



**B. Hemoglobin - multiple ascending doses**



**C. Oxfendazole - single dose, fasted state**



**D. Oxfendazole - single dose, fed state**

